Dude, Where's My Stitch?

Strength Analysis of Absorbable Sutures via COMSOL

BEE 4530: Computer Aided Engineering: Application to Biomedical Processes

Owen Dong
Jonathan Kaufman
Supriya Kumar
Liana Mari

May 2, 2013

Table of Contents

Executive Summary

A common method in aiding postoperative tissue healing is the use of a suture, which functions by holding tissues together. The ideal suture is able to lose strength at the same rate that the tissue gains strength. Absorbable sutures have been studied to provide that strength for the tissue, while at the same time reducing tissue trauma caused by the gradual absorption of the biocompatible material. Because of its excellent fiber-forming ability and biodegradability, polyglycolic acid (PGA) has been investigated for developing resorbable sutures [1]. A computational model of the decomposition and mechanical analysis of this suture provided insight into how the mechanical strength of the suture changes as it deteriorates.

In this novel study, we aimed to create a model via COMSOL that would simulate the degradation of a dissolvable suture and analyze the sutures changing mechanical properties during degradation. Diffusion of water into the suture occurs so quickly that we realized that bulk erosion, not surface erosion, was the main means of degradation. We created a model that simulated the effect of the natural decomposition of the PGA suture within the body via bulk erosion. By decreasing the volume and applying a uniaxial load to the model, we related the effective Young's modulus to the original Young's modulus of the material as the suture degraded.

Suture decomposition rate was determined from scientific literature and previous experiments. The suture's effective elastic modulus decayed with time as the suture dissolved and was absorbed by the body. Knowing the rate at which the elastic modulus decays will allow us to predict the point in time at which the suture no longer holds the tissues together. Findings on the change of material properties of the suture over time are a valuable first step for determining the initial elastic modulus of sutures required for certain tissue repair.

1. Introduction

1.1 Background of Absorbable Sutures

Surgical sutures are common medical devices used today to help facilitate the healing process after an injury or surgery by holding soft tissues together [2]. By definition, the suture is a biomaterial device that is either natural or synthetic, entering the body and approximating tissues together depending on the features and conditions of the tissue to be sutured [3]. Sutures are categorized into two types based on material: nonabsorbable and absorbable. Nonabsorbable sutures are often used for closing surface lacerations, especially those under tension. Absorbable sutures are composed of a biodegradable material and are used when removal of the suture would be difficult or when the wound is in internal body tissues [4]. Unlike traditional sutures, absorbable sutures are broken down by enzymes in the body into soluble material by hydrolytic degradation and bulk erosion.

1.2 Research Review

Different wounds and surgeries induce varying recovery times. Ideally, the wound heals at the same rate that the suture weakens. If a suture does not have the appropriate strength, it will break during surgery or postsurgery. Postsurgery breakages may lead to loss of wound closure and infection [5]. It is of no surprise, then, that both strength and mass degradation are areas that have been studied extensively. The parameters that affect both strength and mass degradation include, but are not limited to initial material composition, initial radius, temperature, and placement in the body. Changes in these parameters lead to changes in the mechanical properties of the suture [6].

Polyglycolic Acid (PGA) is a commonly used composition of sutures found in commercial products such as Dexon and Maxon. PGA undergoes degradation in two phases; first, water diffuses into the suture, and second, the presence of water causes the suture to undergo bulk hydrolytic erosion [7]. Bulk erosion occurs at all surfaces of the suture exposed to water after initial diffusion occurs.

As the suture degrades, it loses its original strength. In Figure 1.1 below adapted from Reed, the percentage of strength remaining in a suture with respect to time is graphed [6]. The strength remaining was determined from in vitro tensile testing of four different suture materials.

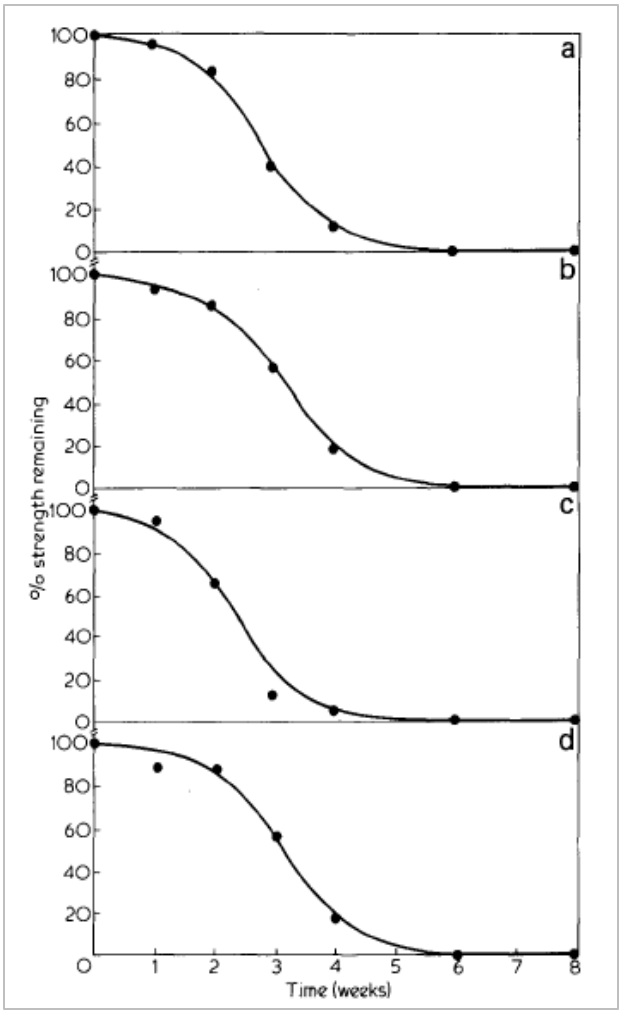

Figure 1.1: *A graph showing the percentage of strength remaining in a suture with respect to time, adapted from [6]. In-vitro tensile data, Dexon^R sutures, (PGA) (Degraded at pH 7 and 37° C). (a), '0' Dexon^R; (b), '0' Dexon^R 's'; (c),'30' Dexon^R; (d),'30' Dexon^R 's'.*

As shown in Figure 1.1, the behavior of percent strength remaining was relatively similar for all suture materials tested. About eighty percent of the initial tensile strength of the PGA suture is retained for two weeks [6]. This allows sufficient time for collagen synthesis required for reinforcement of the fibers. After this two week period, suture strength drops to about twenty percent of its original strength. Nearly all strength is lost six weeks after surgery [6].

The trend of percent mass remaining as a function of time can be seen in Figure 1.2 below. Results for two different suture materials were graphed.

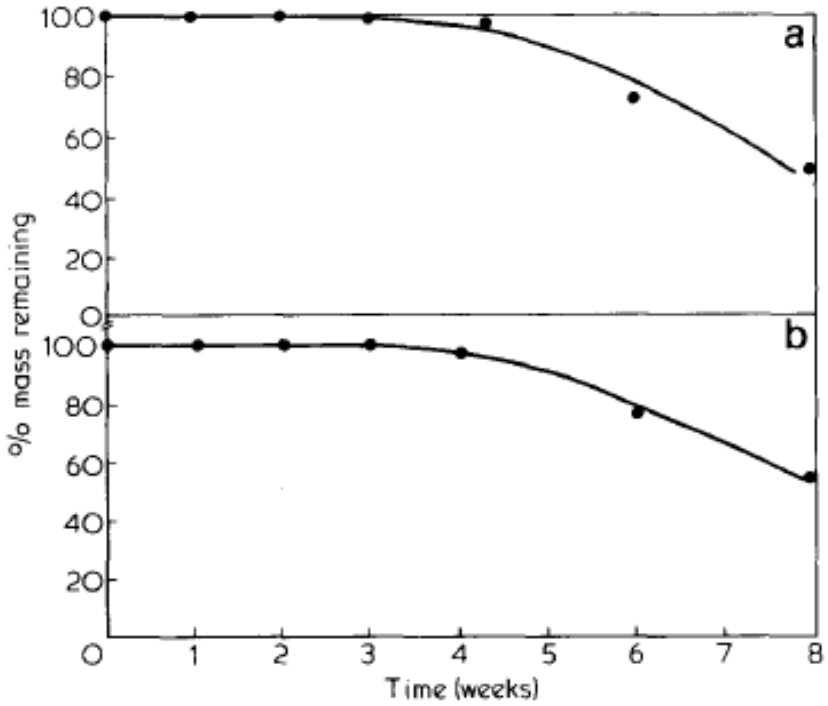

Figure 1.2: *In vitro mass loss data, Dexon sutures, adapted from [6] (Degraded at pH 7 and 37ºC). (a) '0' Dexon; (b), '0' Dexon 's'.*

Figure 1.2 shows that four weeks after surgery, the mass of the suture finally begins to decrease [6]. Interestingly, mass loss is not directly correlated with tensile loss. Even though almost all of the strength of the suture is depleted after four weeks, most of the mass of the suture remains. The reason for this may be that even though mass remains, the bonds between suture particles may be severed. The material is there, but the material is not strong. We believe that the strength of the suture is related to the intact bonds.

The strength of the suture is extremely important. Notably, the suture must be able to withstand knotting and the imposed stress when used to bring soft tissues into apposition [5]. Several models have been developed that describe the degradation process of degradable polymers and subsequent mass loss, yet few models developed to describe the mechanical strength loss of the suture after degradation [8]. In addition, the studies that have been reported have lacked reproducibility [5].

The kinetics of hydrolytic degradation of PGA are not fully understood. The hydrolytic degradation is influenced by factors including structure, molecular weight, and composition of the polymer. Additionally, morphology and porosity of PGA, additives, sterilization procedures and other factors influence the hydrolytic degradation [9].

Thus, we have decided to focus on the mechanical strength loss of PGA as it degrades from water-dependent processes.

1.3 Design Objectives for Suture Degradation

Our COMSOL model simulates the degradation of an absorbable suture made out of PGA and performs a strength analysis on the eroding material. The model determines how the volume, material Young's modulus, and an applied uniaxial load affect the effective Young's modulus.

2. Previous Attempts to Model Suture

Before we found an accurate model of our degrading suture, we went through a few deficient models that did not give results that matched previous experiments. In one iteration of our project, we modeled the suture with surface erosion using a shrinking geometry. Degradation took place in two phases: 1) diffusion of water into the suture and 2) hydrolysis reaction which is a function of water concentration.

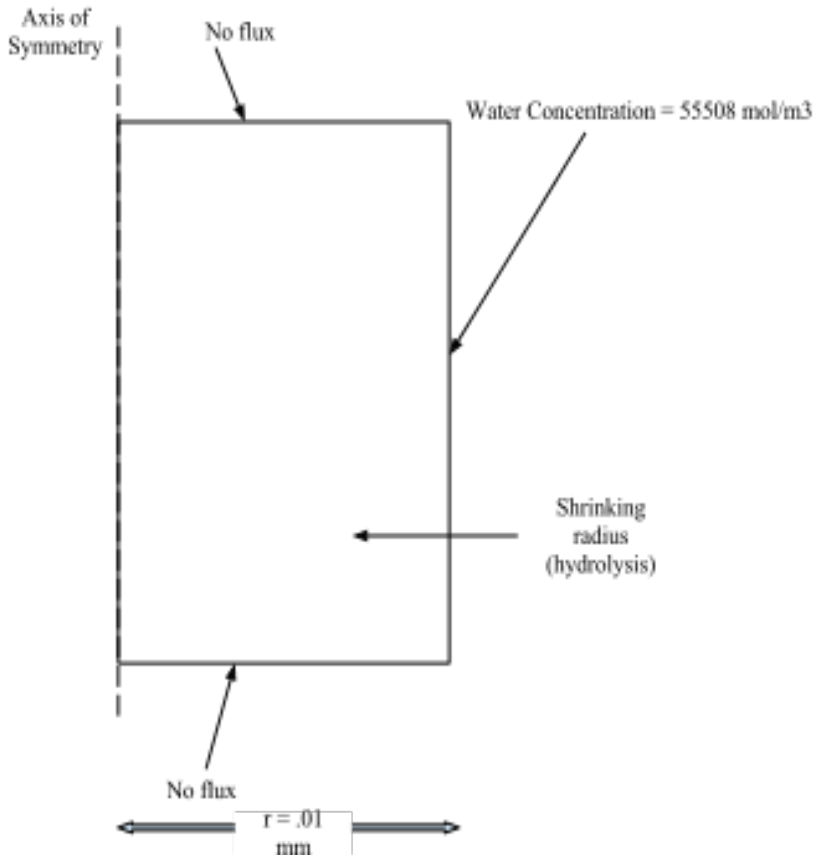

Figure 2.1: *Schematic of boundary conditions for hydrolysis of suture.*

The schematic for this initial model design is depicted in Figure 2.1 above. The model is 2D axisymmetric with the left boundary acting as the axis of symmetry. Water diffused into the suture from the right boundary as the radius shrunk by means of a moving mesh. The hydrolysis occurred only in the radial direction. A constant water concentration was set at the right boundary. A no flux boundary condition was imposed on the upper and lower boundaries.

Obtaining equations that correctly modeled the physical deterioration of the sutures proved to be extremely difficult. We used the following governing equations found in literature [7]:

Diffusion of water:

$$\delta c_w/\delta t = D(\delta^2 c_w/\delta r^2) \quad \text{(Eq. 2.1)}$$

Hydrolysis:

$$\delta c_s/\delta t = kEc_w c_s = \mu_m c_s \quad \text{(Eq. 2.2)}$$

where,

c_w	concentration of water
D	diffusivity
c_s	concentration of carboxyl groups
K	hydrolysis kinetic constant
E	concentration of ester groups
μ_m	hydrolysis rate

The velocity of the mesh is based on the change in mass of carboxyl groups over time. The mesh only moves inward in the r-direction. The velocity at the boundary of the suture was calculated by taking the derivative of the mass of carboxyl divided by the product of density of the carboxyl groups and circumferential surface area of the stitch with respect to time.

$$v_{mesh} = \frac{\partial(m_{carboxyl}/\rho_{carboxyl}A_{surface})}{\partial t} \quad \text{(Eq. 2.3)}$$

While the results we received were an accurate representation of the equations and theory we presented, they revealed that many of our initial assumptions were incorrect. Figure 2.2 below depicts the suture concentration after 50,400 seconds. Figure 2.3 below shows how the suture radius degrades over time. Because our velocity was indirectly based on the water diffusion (which occurred extremely fast), the radius size was reduced too quickly. This model proved to be inadequate for our purposes.

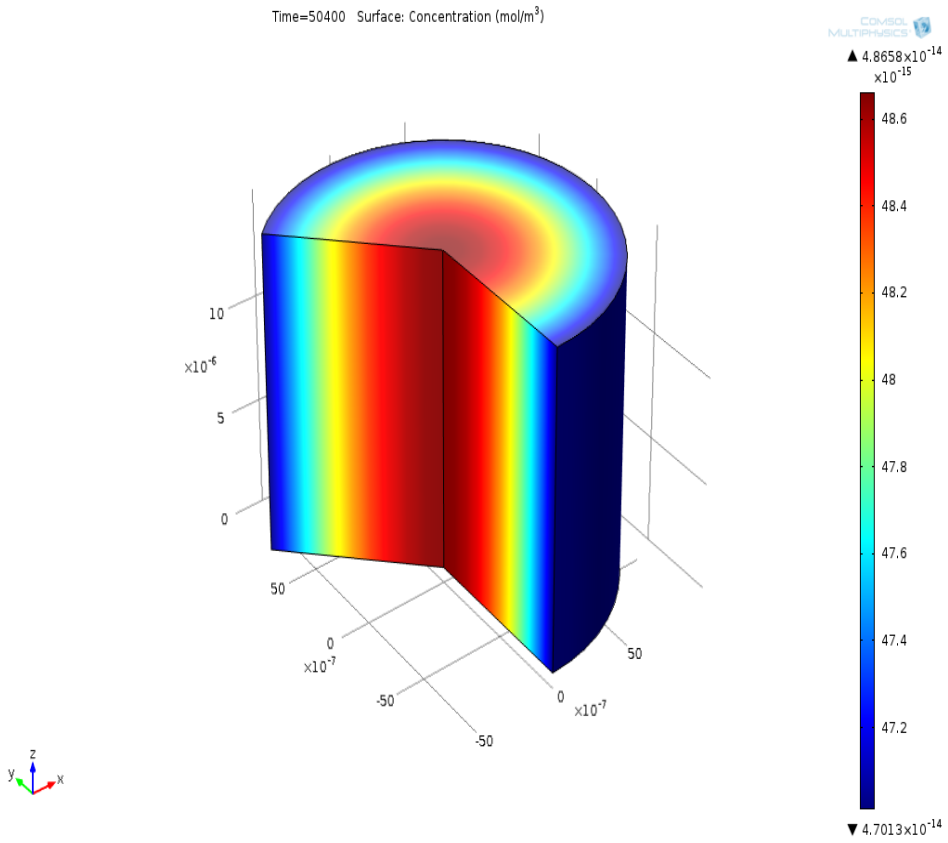

Figure 2.2: *3-D model of diffusion of suture concentration in the suture.*

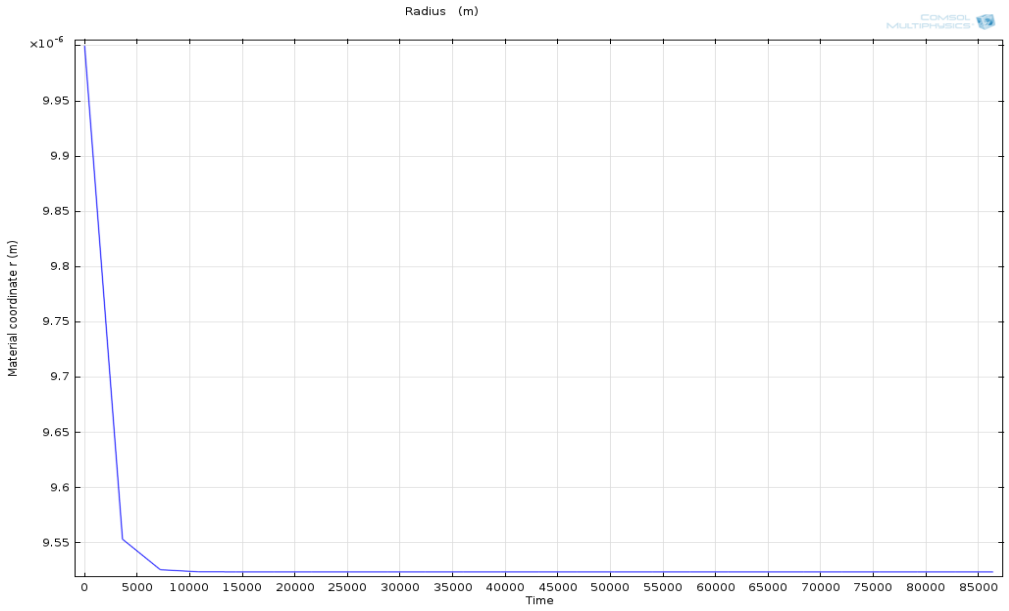

Figure 2.3: *Suture radius vs. time after diffusion of water into suture and hydrolysis.*

3. COMSOL Implementation Methods

3.1 Schematic of Suture

From our initial model of the suture as a shrinking geometry, we found that the diffusion of water was much faster than the suture degradation by hydrolysis. Thus, we decided to focus on bulk erosion rather than surface erosion. We modeled this bulk erosion as a decrease in suture volume based on the increase in radius of pores or void area. Now, our model mainly analyzed the mechanical strength of the suture based on its decreasing volume.

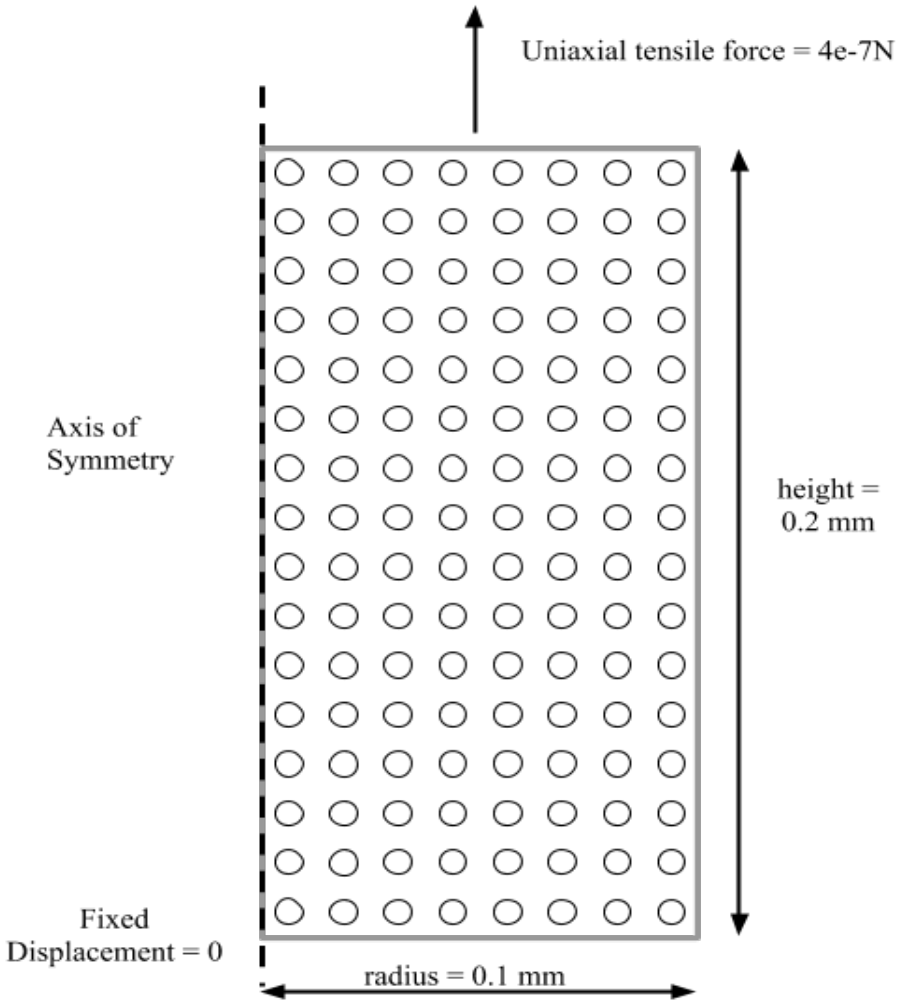

Figure 3.1: *Suture geometry showing boundary conditions. The left boundary has an axisymmetric boundary condition. The right boundary is a free surface. The top boundary has a uniform axial load of 4E-7 N applied across it. The bottom boundary condition is fixed. The right boundary is free.*

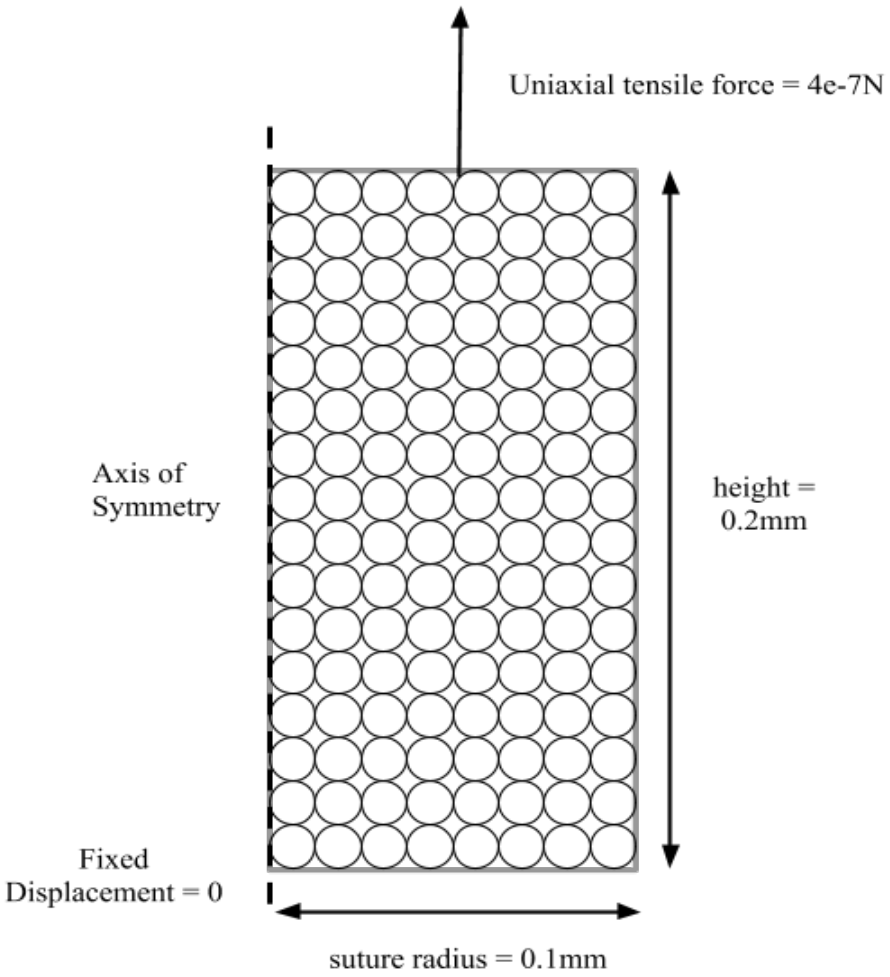

Figure 3.2: *Suture geometry deformation at a later time. The size of the holes increases because of degradation effects of the body on the suture.*

As Figure 3.1 and 3.2 show, the model is 2D axisymmetric. After initial hydrolysis, the suture deteriorates at any surface. The deterioration that occurs after hydrolysis was modeled by eleven different geometries where only the radius of the hole size varied to mimic the degradation of the suture by bulk erosion. The eleven different models had pore radii that ranged from 0 to 3 μm in steps of 0.3 μm. Each geometry was a snapshot of a specific time during the suture decomposition. The method to relate pore radius and time is discussed later on in Section 4.

3.2 Mechanical Analysis Equations

We modeled the suture as a linear elastic material. Hooke's law applies:

$$\sigma = E\varepsilon\,, \qquad \text{(Eq. 3.1)}$$

where σ is stress, E is Young's modulus, and ε is strain. The applied load is normalized by area to obtain stress by the following formula:

$$\sigma = F/A\,, \qquad \text{(Eq. 3.2)}$$

where F is the applied force and A is the cross-sectional area. The stress throughout the body will change when the cross-sectional area, A, changes. The force is kept constant, so as the area decreases (more porous area), the stress will be higher in that part of the suture.

The z component of the spatial stress tensor and the z component of the material strain tensor were selected for computation by COMSOL. These calculations were done for each of the eleven snapshot models. Homogenization of the numerous values calculated by COMSOL resulted in an average stress and an average strain over the entire suture domain. These averages were used to compute an effective Young's modulus.

$$E_{eff} = \frac{\sigma_{average}}{\epsilon_{average}}\,, \qquad \text{(Eq. 3.3)}$$

3.3 Boundary and Initial Conditions

The boundary conditions are shown in Figure 3.1 and Figure 3.2. This problem is modeled in 2D to show deformations caused by tensile loading in both the radial (r) and height (z) direction. The left boundary has an axisymmetric boundary condition. The suture-tissue interface on the right boundary is a free surface. The top boundary has a uniform axial load of 4E-7 N applied across it. The applied load is very small in order for COMSOL to calculate strains. The force is somewhat arbitrary because as long as some strain is created in the model, the effective Young's modulus can be calculated. The bottom boundary condition is fixed. All other domains are free. Initial displacement and structural velocity are zero in all directions.

3.4 Mesh

Our final mesh used the preset "coarser" free triangular mesh setting for a total of 30678 elements (Figure 3.3). This mesh was chosen after we performed mesh convergence which is described below.

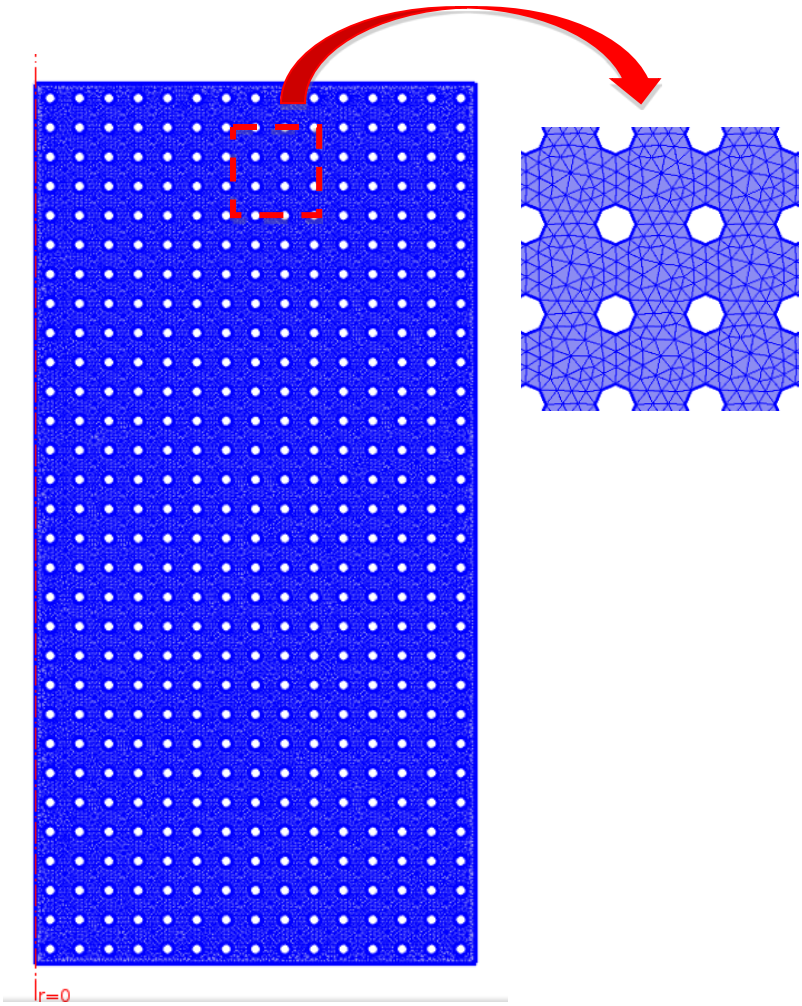

Figure 3.3: *Coarser mesh with 30678 elements. This mesh was determined by mesh convergence with regard to effective modulus.*

3.5 Mesh Convergence

A mesh convergence analysis (Table 3.1) was performed to determine the optimal mesh for use with our results. The optimal mesh has enough elements to avoid discretization errors and minimizes computing power usage. The solution becomes independent of mesh size once the mesh is converged. The parameter we tracked was the new effective Young's modulus (E_eff) of the suture after six weeks (approximate duration of time over which the suture is effective). The model had a pore radius of 1.5 μm. The values of E_eff were calculated for five preset COMSOL mesh sizes from extremely coarse to normal.

Table 3.1: *Mesh Convergence of Free-Triangular Model for Suture Degradation*

Mesh Size	Number Elements	E_eff (GPa)
Extremely Coarse	6326	5.577682312
Extra Coarse	8200	5.58743039
Coarser	30678	5.544980111
Coarse	91720	5.543654203
Normal	174860	5.543569345

The results of the mesh convergence suggest that E_eff asymptotes at approximately 5.545 GPa (Figure 3.4). We chose the *coarser* mesh with 30,678 elements because the mesh begins convergence at this point, and the tradeoff between solution accuracy and computation time is balanced.

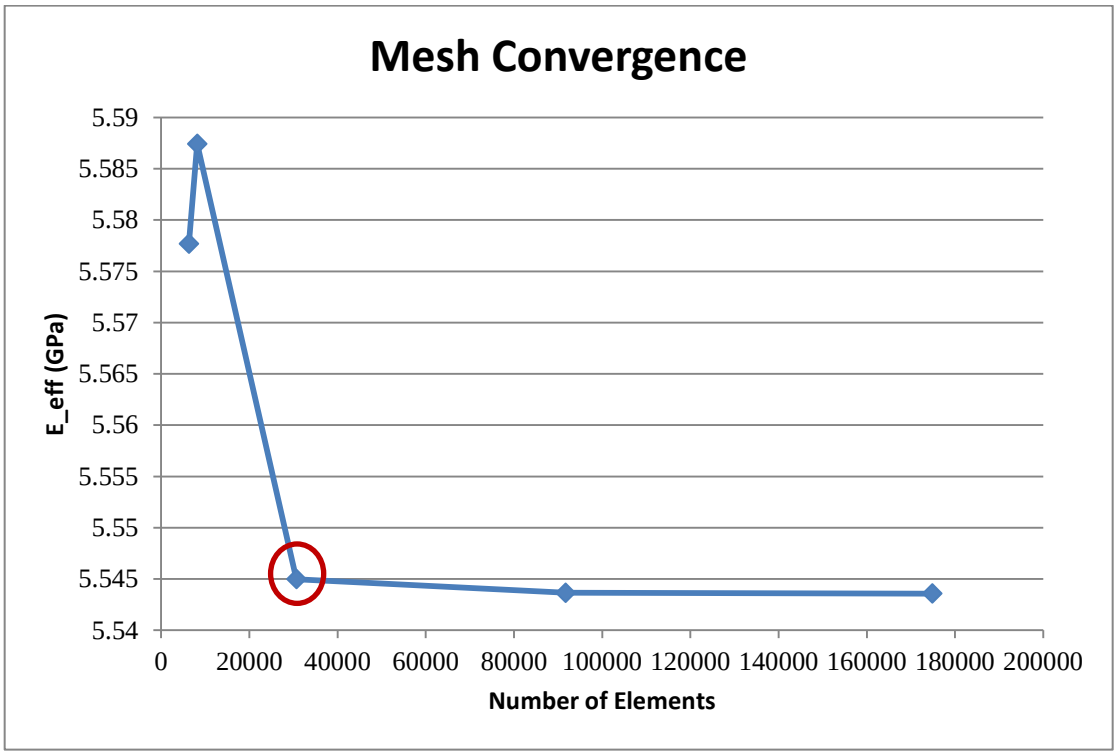

Figure 3.4: *Mesh Convergence Analysis. The suture effective elastic modulus was plotted against the number of elements in the mesh after six weeks. E_eff converges at approximately 30678 elements as shown on the graph by the red circle. The solution becomes independent of mesh size as mesh size increases beyond this point.*

4. Complete Solution and Results

For each of the eleven selected pore radius sizes (ranging from 0 to 3 μm in steps of 0.3 μm), COMSOL returned values for the suture volume fraction, average stress, and average strain. Our COMSOL mechanical analysis of degradable sutures is not time-dependent. Thus in order to describe the amount of time it takes for the pore size to increase, we had to manually pick a time for each radius size that we predetermined in our models based on empirical data shown in Figure 1.2. The volume fraction percentage for the specified radius was equated to the percent mass remaining in Figure 1.2.

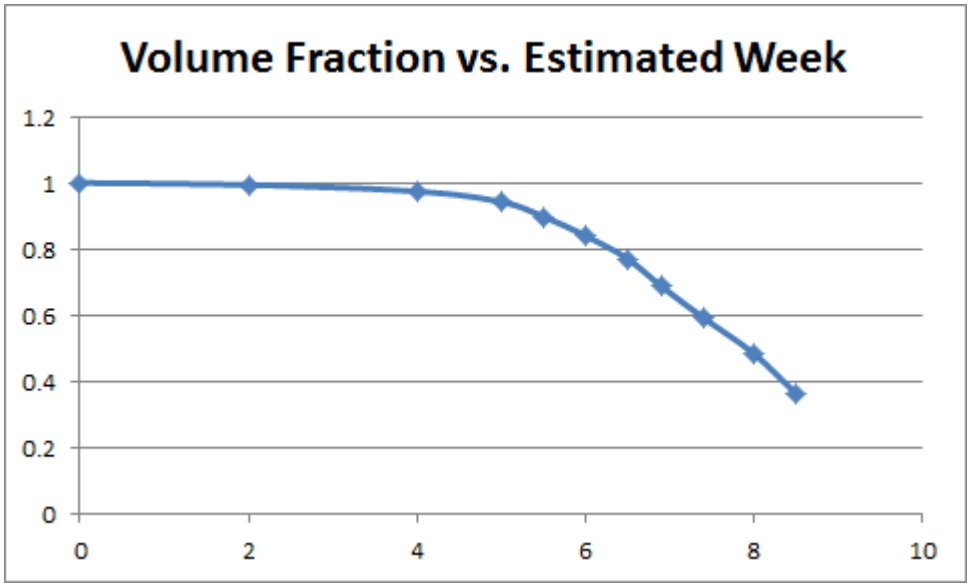

Figure 4.1: *Suture volume fraction degradation over time.*

At later stages, the same time change leads to a larger decrease in volume when compared to an earlier stage because the surface area of the pore is bigger. Therefore, hydrolysis affects a larger portion of the suture and more mass is lost.

2D Strain Models

Figure 4.2 illustrates the strain fields in the suture for various volumes. The volume changes as the suture dissolves. The pictures progress from time zero to the time when volume is 35% initial volume. Initially, the suture experiences relatively little strain because the bonds are fully intact. As time progresses, the strain throughout the suture increases due to increased stresses induced from the loading condition. There is a high strain concentration at the lower right hand corner at earlier stages of degradation. We believe the concentration occurs because of the imposed boundary conditions. The bottom right corner is the freest part of our model because the right

boundary is free and the bottom boundary is fixed. The strain concentration diminishes as the volume fraction decreases.

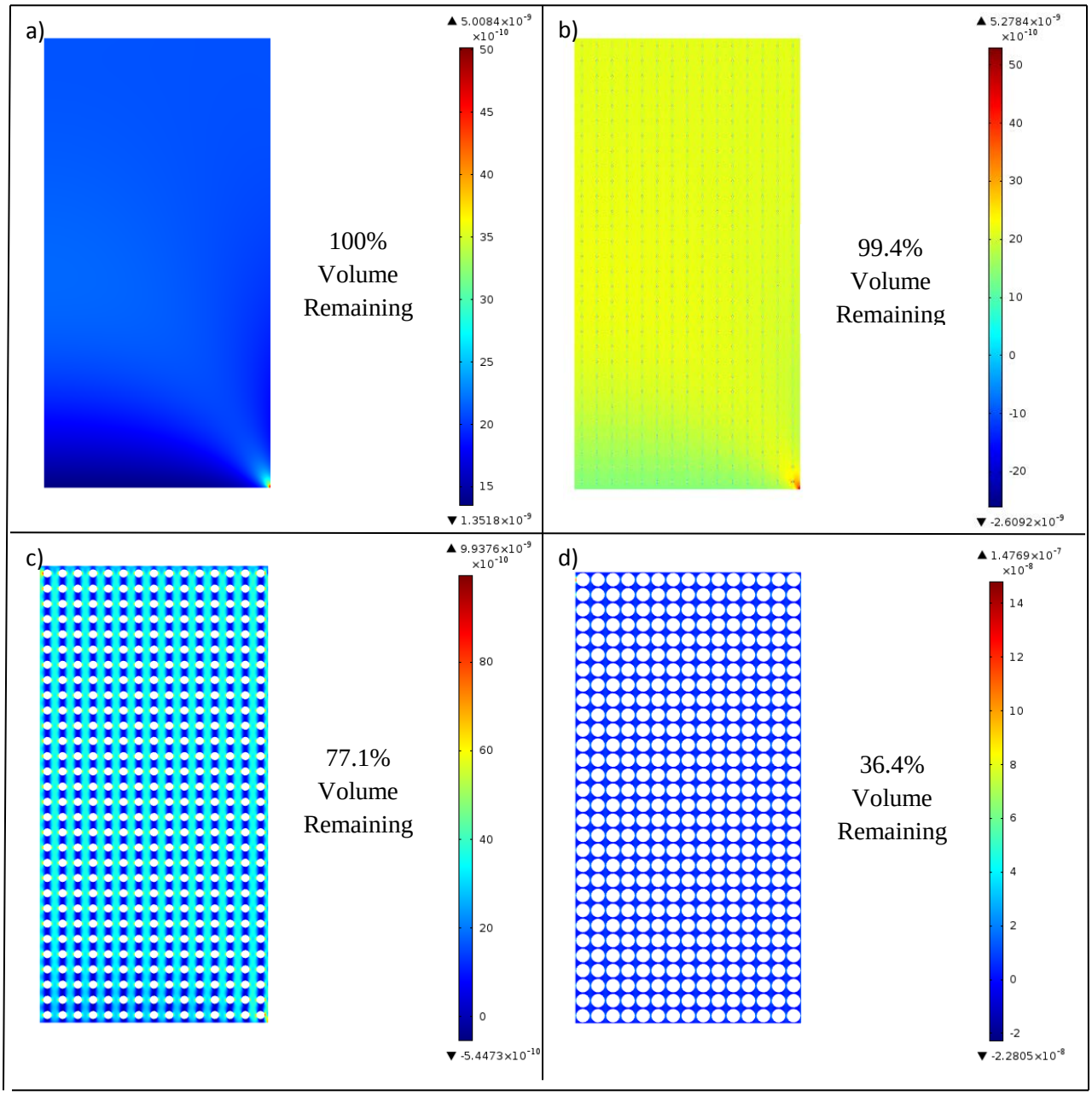

Figure 4.2: *Images showing the strain throughout the suture at different weeks. (a), R_{hole}=0, week 0, (b), R_{hole}=0.3µm, week 2, (c) R_{hole}=1.8 µm, week 6.5, (d), R_{hole}=3µm, week 8.5.*

2D Stress Models

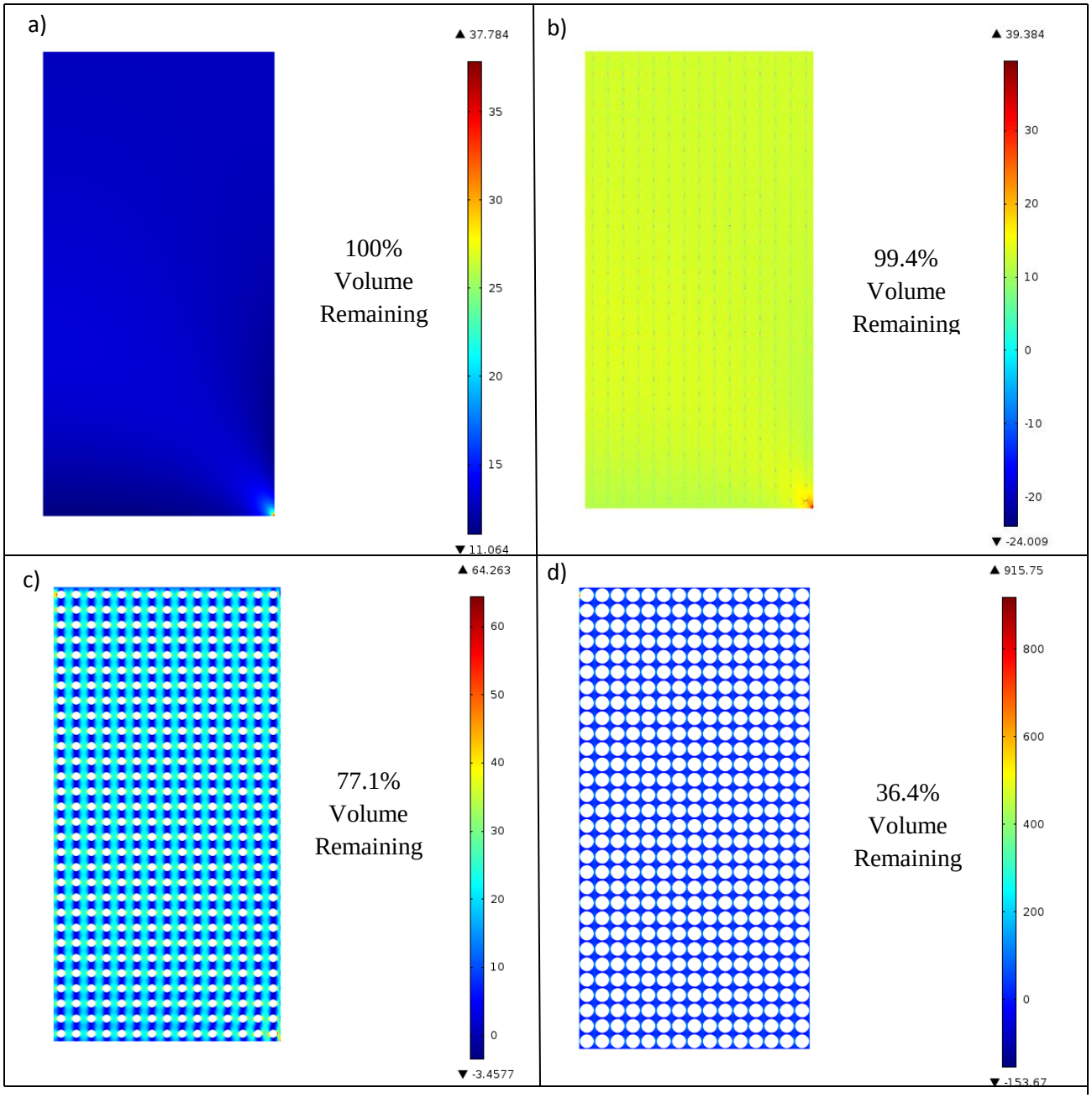

Figure 4.3: *Images showing the stress throughout the suture at different weeks. (a), R_{hole}=0, week 0, (b), R_{hole}=0.3µm, week 2, (c) R_{hole}=1.8 µm, week 6.5, (d), R_{hole}=3µm, week 8.5.*

Figure 4.3 illustrates the stress fields in the suture for various volumes. The volume changes as the suture dissolves. Similar to the strain results, the suture experiences relatively little stress initially because the bonds are fully intact. As can be seen by the scales, the stress within the suture increases as time progresses. The maximum and minimum values for the range of stress change with each new week (or change in pore radius size) because the same load applied to a

domain with lower volume fraction will result in a higher stress than when applied to a domain with a larger volume fraction.

The behavior of a linear elastic material can be described by Hooke's law. Stress over strain is the elastic modulus of a linear elastic material. Since the average Young's modulus is constant, the decrease in effective Young's modulus is mostly due to the volume decrease of the suture. Figure 4.4 below depicts the decrease in effective modulus of the degrading suture compared to the initial elastic modulus. The effective modulus decreases at a higher rate at larger pore radius sizes because of the lower volume fractions.

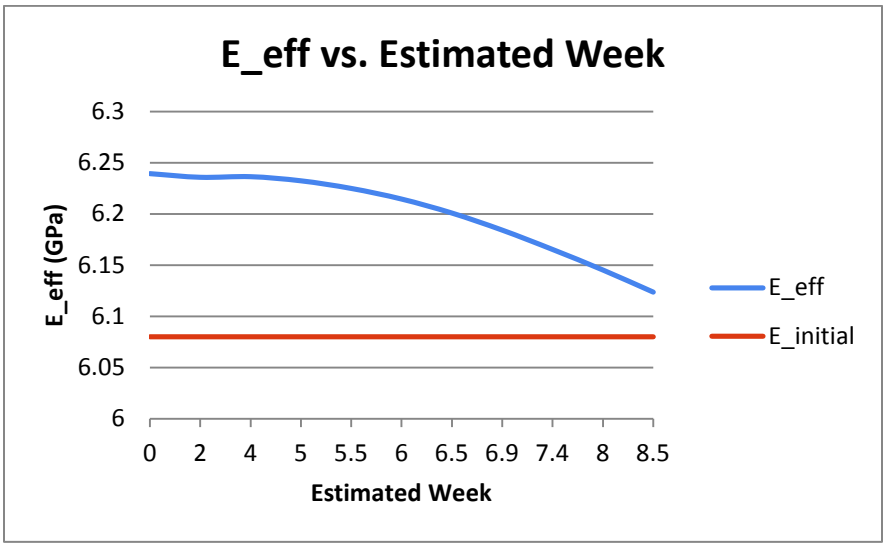

Figure 4.4: *Comparison of Young's Modulus of initial suture to effective Young's Modulus of degraded suture.*

The data for the graphs in this section are displayed below.

Table 4.1: *COMSOL Output Properties for Suture Degradation*

Estimated Week	Pore Radius (um)	Volume Fraction	E_eff (GPa)	Stress	Strain
0	0	1	6.23945	12.7324	2.04063E-09
2	0.3	0.99423	6.20283	12.80631	2.05365E-09
4	0.6	0.97456	6.08	13.06479	2.0949E-09
5	0.9	0.94275	5.87533	13.50625	2.16709E-09
5.5	1.2	0.89822	5.5914	14.17516	2.27714E-09
6	1.5	0.84097	5.22628	15.14019	2.43623E-09
6.5	1.8	0.77099	4.78087	16.5143	2.6632E-09
6.9	2.1	0.68829	4.25657	18.49846	2.99123E-09
7.4	2.4	0.59287	3.65526	21.47569	3.4833E-09
8	2.7	0.48473	2.97881	26.26686	4.27433E-09
8.5	3	0.36384	2.22806	34.99405	5.71457E-09

5. Accuracy Check

There is relatively little published data on the decreasing elastic modulus of sutures as they dissolve. We were able to find information on the percent of strength remaining and percent mass remaining in the suture over time. We matched the volume fraction remaining in our model to the time that the equivalent volume remained in the Reed's experiments [6]. Our results are solely based on empirical data that was found in literature. In order to give our mechanical analysis more legitimacy and reason, we tried to find a chemical reaction basis for the chosen times for each volume fraction calculated by COMSOL. Tang, et. al described the "chemical reaction kinetics of ester bonds in degradable polymers such as PGA" by the following equation:

$$\frac{dM}{dt} = -\lambda M \qquad \text{(Eq. 5.1)}$$

where M = molecular weight of the polymer and λ is the degradation rate [8].

From this equation we derived an equation relating volume fraction, V_{frac} to time t and the degradation rate λ:

$$V_{frac} = e^{-\lambda t} \qquad \text{(Eq. 5.2)}$$

We plotted V_{frac} vs. t using literature's value for degradation rate, $\lambda = 0.0117\ day^{-1}$ and compared it to our volume fraction vs. estimated time (Figure 5.1).

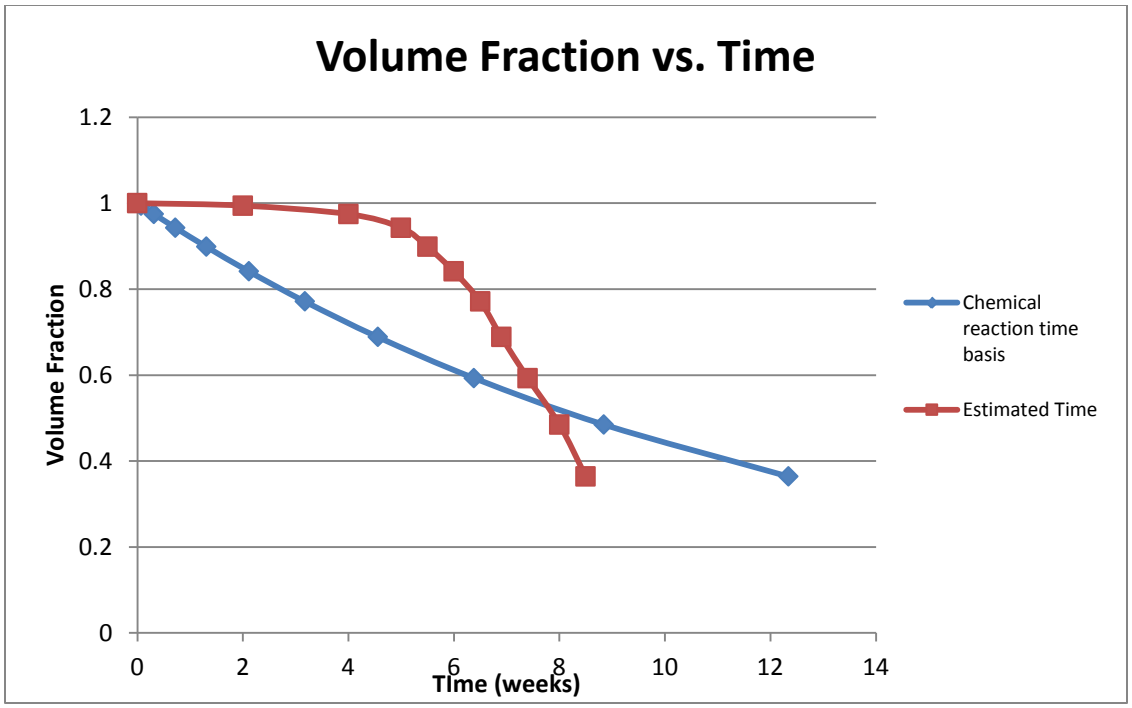

Figure 5.1. *Suture volume fraction vs. time for both the chemical reaction kinetics and the mechanical empirical data methods.*

From Figure 5.1, we can conclude that the chemical reaction kinetics graph is very different from and thus does not validate our results. Suture strength experimentation is minimal, so another accuracy check would be common sense. Our results show that strength decreases with time. Even if our time values are not exact, they seem to match up with what one would expect in the real world.

6. Sensitivity Analysis

Sensitivity of our model was assessed based on a parameter's change on the effective Young's modulus. We varied both the initial Young's modulus of the suture and the suture density as shown in Figure 6.1.

Note that as we increase the initial Young's modulus the effective modulus also increases. Figure 6.1a shows that the initial Young's modulus is important in selecting the proper suture because E_{eff} varies depending on the initial modulus. Additionally, note that E_{eff} is unaffected by the density as shown in Figure 6.1b. The value of the effective modulus does not change because E_{eff} is a function of stress and strain which are independent of density.

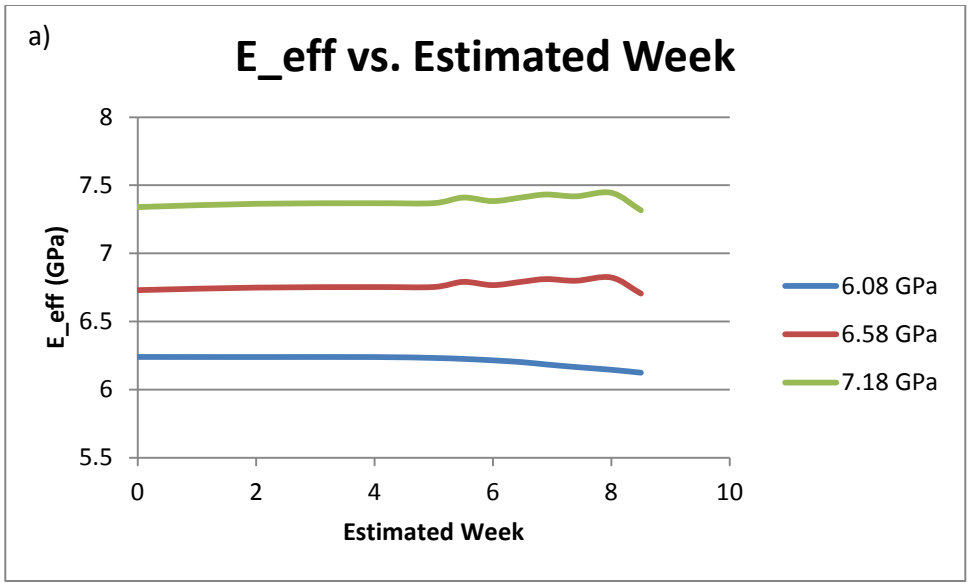

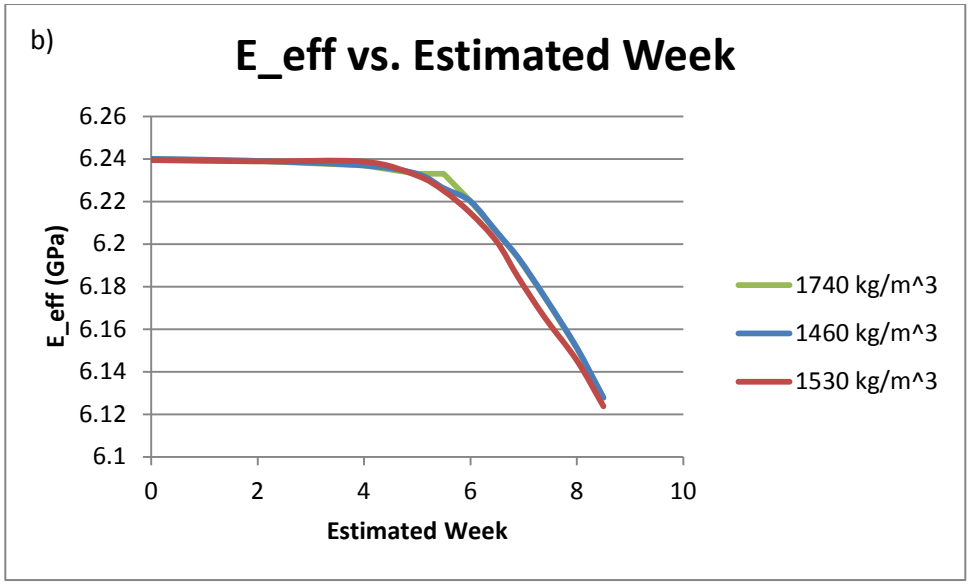

Figure 6.1: *Sensitivity Analysis of (a) initial Young's Modulus and (b) PGA density.*

Not pictured is the sensitivity analysis on the radius of the suture. This is because, like density, it does not affect the outcome of E_{eff}.

7. Conclusions

Our model showed that the effective Young's modulus of a suture decreases as it dissolves by bulk erosion. These results allow surgeons to choose the appropriate suture material with the appropriate mechanical properties (initial Young's modulus) for different procedures and parts of

the body. The surgeon can determine the strength the suture must retain to be effective in the applied area.

We looked at several ways to model the degradation of a suture. Although each method accurately depicts a portion of the degradation, the entire process is not captured by a single model. In the future, a method that considers both the mechanical and chemical breakdown of the suture should be explored further.

8. Limitations

Our model geometry is obviously simplified. A more realistic model would be a three dimensional model with spheres that represent the pores. Further, all the pores would not be the same size.

Also, the homogenization of stress and strain to obtain a Young's modulus is not the most accurate way to calculate this value. Instead, the highest stress should be considered because that would be where the suture would deform the most. We want to know a worst-case scenario.

Our model is not a realistic depiction of the degradation of the suture strength because it does not change much over time. Although this is not an accurate model, like our last one, it is a step towards finding the correct model of suture degradation. Since this is only a semester-long course, we were not able to continue our investigation of this process. Given additional time, we would have been able to explore a combination of the proper geometry and physical and chemical mechanisms by which the degradation actually takes place.

Appendix:

Table A1: *Input Parameters*

Parameter	Parameter Name in COMSOL	Value
Stitch Radius [10]	r_stitch	.1e-3m
Height of Stitch	h_stitch	2* r_stitch
Maximum Pore Radius	rmax	.003e-3m
Pore Radius	r0	.5* rmax
Number of Pores in Radial Direction	num_pore_r	15
Number of Pores in z Direction	num_pore_z	30
Pore Center Distance in Radial Direction	r_stitch/num_pore_r	6.666e-6m
Pore Center Distance in z Direction	z_stitch/num_pore_z	6.666e-6m
PGA Density [10]	PGA_density	$1.53g/cm^2$
Young's Modulus [10]	Young	6.08GPa
Applied Load	app_load	4e-7N
Poisson Ratio [10]	pois	.3

References

1. S. Dumitriu, *Polymeric Biomaterials*, 2002.

2. T. H. Witte et al., “A Transducer for Measuring Force on Surgical Sutures,” *The Canadian Journal of Veterinary Research*, vol. 74, pp. 299-304, 2009.

3. C. K. S. Pillai and C. P. Sharma, “Review Paper: Absorbable Polymeric Surgical Sutures: Biodegradability, and Performance,” *Journal of Biomaterials Applications*, vol. 25, pp. 291-366, Nov., 2010.

4. H. Karounis et al., “A Randomized, Controlled Trial Comparing Long-term Cosmetic Outcomes of Traumatic Pediatric Lacerations Repaired with Absorbable Plain Gut versus Nonabsorbable Nylon Sutures,” *Academic Emergency Medicine*, vol. 11, Pg. 730–735, 2004

5. J.A. Von Fraunhofer et al., "Tensile Strength of Suture Materials." *Journal of Biomedical Materials Research*, vol. 19, pp. 595-600, 1985.

6. A. M. Reed and D.K. Gilding, “Biodegradable Polymers for Use in Surgery -- Poly(glycolic)/poly(lactic acid) Homo and Copolymers,” *Polymers*, vol. 22, pp. 494-498, Apr. 1981.

7. A.C. Vieira et al., “Mechanical Study of PLA-PCL Fibers During In Vitro Degradation”.

8. C.Y. Tang et al., “Damage Modeling of Degradable Polymers Under Bulk Erosion.” *Journal of Applied Polymer Science*, pp.2658-2665, Aug., 2012.

9. J. Chen et al., “Time-of-Flight Secondary Ion Mass Spectrometry Studies of Hydrolytic Degradation Kinetics at the Surface of Poly(glycolic acid),” *Macromoleculres*, vol. 33, no. 13, pp. 4726-4732, 2000.

10. C.C. Chu et al., *Wound Closure Biomaterials and Devices.* Boca Raton, Florida: CRC Press LLC, 1997.